



# New Schiff Base and Its Platinum Complex: Inhibition of Amyloid Aggregation

## *Yeni Bir Schiff Bazı ve Platin Kompleksi: Amiloid Agregasyonunun İnhibisyonu*

Özge Özcan , Salih Günnaz , Sevil İrişli\* 

Ege University, Faculty of Science, İzmir, Türkiye

### Abstract

This study investigates the synthesis and characterization of a Schiff base (L) comprising amine and imine donor atoms, specifically N1-(4-(benzyloxy)benzylidene)-N2-phenylethane-1,2-diamine, along with its Platinum(II) complex (Pt-L). The structural elucidation of both the ligand and complex is accomplished through various spectroscopic techniques including Fourier-transform infrared spectroscopy (FT-IR), proton nuclear magnetic resonance ( $^1\text{H-NMR}$ ), carbon-13 nuclear magnetic resonance ( $^{13}\text{C-NMR}$ ), and elemental analysis. Furthermore, the potential inhibitory effects of the Pt-L complex on  $\text{A}\beta_{1-42}$  aggregation are explored using the human neuroblastoma cell line (SH-SY5Y) as a model system. The cytotoxicity of the Pt-L complex on SH-SY5Y neuroblastoma cells is examined, revealing an  $\text{IC}_{50}$  value of 19.22  $\mu\text{M}$ . The inhibition kinetics of  $\text{A}\beta$  aggregation are also investigated fluorometrically using Thioflavine-T. By analyzing the area under the curve, it is calculated that the complex (1.0:1.0 molar ratio) interacts with amyloid at a rate of 65%. These results obtained in our study show that the complex is promising in terms of inhibition of  $\text{A}\beta_{1-42}$ .

**Keywords:** Anti-Alzheimer activity, cytotoxicity, schiff base, platinum-schiff base complexes.

### Öz

Bu çalışma, amine ve imin donör atomlarını içeren bir Schiffbazı (L) bileşiğinin sentezini ve karakterizasyonunu incelemektedir. Özellikle, N1-(4-(benziloksi)benziliden)-N2-feniletan-1,2-diamin bileşiği ve onun Platin(II) kompleksi (Pt-L) üzerinde durulmaktadır. Hem ligandın hem de kompleksin yapısal aydınlatılması, Fourier-dönüşümlü kızılötesi spektroskopi (FT-IR), proton nükleer manyetik rezonans ( $^1\text{H-NMR}$ ), karbon-13 nükleer manyetik rezonans ( $^{13}\text{C-NMR}$ ) ve elementel analiz gibi çeşitli spektroskopik teknikler kullanılarak gerçekleştirilmiştir. Ayrıca, Pt-L kompleksinin  $\text{A}\beta_{1-42}$  agregasyonu üzerindeki potansiyel inhibisyon etkileri, insan nöroblastoma hücre hattı (SH-SY5Y) kullanılarak bir model sistem olarak araştırılmıştır. Pt-L kompleksinin SH-SY5Y nöroblastoma hücreleri üzerindeki sitotoksitesi de incelenmiş ve  $\text{IC}_{50}$  değeri 19.22  $\mu\text{M}$  olarak belirlenmiştir.  $\text{A}\beta$  agregasyonunun inhibisyon kinetiği ayrıca Thioflavin-T kullanılarak florometrik olarak incelenmiştir. Eğrinin altında kalan alanın değerlendirilmesi ile kompleksin 1.0:1.0 mol oranında amyloid ile %65 oranında etkileştiğini göstermiştir. Çalışmamızda elde edilen bu sonuçlar, kompleksin  $\text{A}\beta_{1-42}$  inhibitörü olarak umut verici bir bileşik olduğunu göstermektedir.

**Anahtar Kelimeler:** Anti-Alzheimer aktivitesi, sitotoksite, schiff bazları, platin-schiff bazı kompleksleri.

## 1. Introduction


Schiff bases are considered one of the most versatile classes of bioactive compounds due to their capacity to interact with various elements (Garai et al. 2018, Pal et al. 2020). Schiff bases and their metal complexes are widely used in

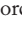
many biological fields such as anticancer, antiviral, anti-inflammatory, antifungal, etc. (Liu et al. 2014, Rao et al. 2013, Mohammed et al. 2022).

Neurodegenerative diseases (ND) are chronic and progressive disorders that share many common features. The accumulation of death-causing protein aggregates (Especially  $\text{A}\beta_{1-42}$ , amyloid beta(1-42)) in certain areas of the brain causes damage and results in memory loss (Ross and Poirier 2004, Soto and Pritzkow 2018). In Alzheimer's disease (AD), the alteration in the nerve transmission with nerve cell death is recorded by the presence of neurofibrillary tangles with phosphorylated forms of the tau protein as a microtubule protein. Studies have been carried out for the future of

\*Corresponding author: [sevil.irisli@ege.edu.tr](mailto:sevil.irisli@ege.edu.tr)

Özge Özcan  [orcid.org/0009-0008-1243-2552](https://orcid.org/0009-0008-1243-2552)

Salih Günnaz  [orcid.org/0000-0002-7422-6593](https://orcid.org/0000-0002-7422-6593)

Sevil İrişli  [orcid.org/0000-0002-3727-2216](https://orcid.org/0000-0002-3727-2216)



Alzheimer's disease, which is based on the assumption of metal ions in the treatment of Alzheimer's disease (Kepp 2017). In this context, metal ions, especially copper, play an important role. It should be noted that copper, iron and zinc ions also participate in various essential components in the functions of the body. When copper accumulates as a toxic cation, it also contributes significantly to Alzheimer's disease by increasing the aggregation of  $A\beta_{1-42}$  (Gaetke et al. 2014). For this reason, diamine-based pharmacophore chelators have been synthesized using aromatic or alkyl amine/imine groups (Santos et al. 2016). It is important to synthesize ligands by taking into account some pharmacophore groups of pro-drug chemicals that can be used in the treatment of AD (Palanimuthu et al. 2017). Studies on the inclusion of two nitrogen-containing compounds as chelating groups in molecules for the removal of metal ions that play a role in aggregation such as Cu and Zn have gained importance.

Another approach is the use of metal complexes that can remove metal from  $A\beta_{1-42}$  in case of disease or modulate  $A\beta$  aggregation to prevent disease (Rowinska-Zyrek et al. 2015). Based on this idea, Pt-based metal complexes were synthesized and their inhibition activities on  $A\beta_{1-42}$  were investigated (Liu et al. 2018). In the metal complexes formed with these ligands, the metal mostly interacts with the histidine nitrogens of amyloid, and the pharmacophore groups of the ligand can also contribute to this interaction (Valensin et al. 2012). Although Pt has generally been used in studies on this subject, especially in recent years, there have been studies including Ru, Ir and Pd complexes (Khan et al. 2024). There are limited studies on Schiff base-metal complexes (Heffern et al. 2014, Roberts et al. 2020, Iscen et al. 2019).

In the study, new platinum(II)-schiff base complex (Pt-L) which has new Schiff base (L) containing amine/imine groups was synthesized. The structures of the synthesized compounds were determined by spectroscopic methods. Ligand synthesis was planned by taking into account the groups (pharmaphores) in some drugs used in the treatment of AD (Palanimuthu et al. 2017). We aimed to prevent aggregation by binding studies of these synthesized substances. In vitro study of the complex was performed on the human neuroblastoma cell line (SH-SY5Y), and cytotoxicity tests were performed beforehand. The inhibition kinetic of Thioflavin T fluorescent aggregation of complex was measured by the method.

## 2. Material and Methods

### 2.1. Chemicals

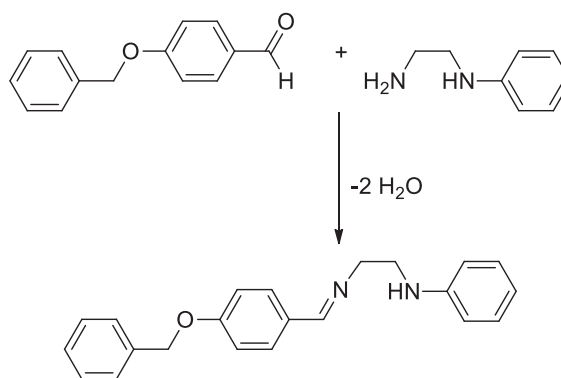
The reagents  $K_2PtCl_4$ , 4-Benzyloxybenzaldehyde, methanol, chloroform, dichloromethane, and diethyl ether used in the synthesis were commercially purchased from Sigma Aldrich, and solvents were purified according to standard methods (Haas 1971).  $Pt(DMSO)_2Cl_2$ , used as the starting complex, was synthesized according to the literature (Price et al. 1972). The  $A\beta_{1-42}$  Aggregation Kit for fluorescence studies was purchased from Anaspec.  $A\beta_{1-42}$  (human) for cell studies and AFM were purchased from Bachem.

### 2.2. Instrumentations

Melting points were obtained using an Electrothermal Melting Point detection apparatus. Elemental analyzes were performed Ege University. Infrared spectra were recorded on a Perkin Elmer Spectrum 100 FT-IR spectrophotometer in the range of  $4000-400\text{ cm}^{-1}$  for ligands,  $4000-200\text{ cm}^{-1}$  for complexes.  $^1H$  and  $^{13}C$  NMR spectra were measured at Varian AS 400 MHz spectrometer.  $CDCl_3$  and  $DMSO-d_6$  were used as the solvents and TMS was used as the internal standard. ThT measurements were made using Thermo Fisher Scientific, Varioskan Flash microplate reader device (Temperature  $37^\circ C$ ) with 480 nm excitation and 484 nm emission wavelengths.

### 2.3. Synthesis

#### 2.3.1. Synthesis of (N1-(4-(benzyloxy)benzylidene)-N2-phenylethane-1,2-diamine)(L)

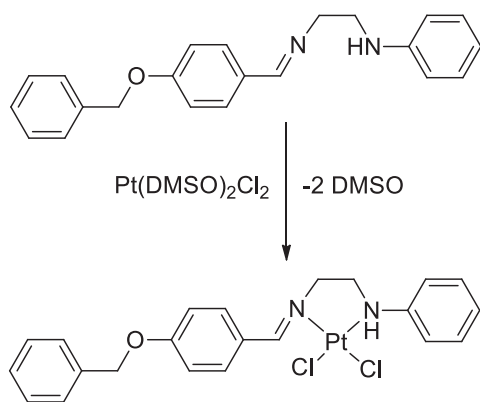


**Scheme 1.** Synthesis pathway for the L.

A solution of 4-Benzyloxybenzaldehyde (15.5 mg, 0.079 mmol) in 2 mL methanol was prepared in a schlenk. Then, N-phenylethylenediamine (0.01 mL 0.079 mmol) solution in 1 mL methanol medium was added dropwise and stirred for 24 hours at room conditions. After 24 hours

in the reaction, a precipitate was formed. The precipitate and filtrate were separated. The precipitate was dried in the vacuum line. Yield: 87.5%, FT-IR (KBr disk,  $\text{cm}^{-1}$ )  $\nu_{\text{C=N}}$  = 1642.  $^1\text{H}$  NMR (400 MHz,  $\text{DMSO-d}_6$ )  $\delta$  (ppm): 8.25 (s, 1H,  $\text{CH=N}$ ), 7.69 (d, 2H,  $J=8.4$  Hz, Ar- $H$ ), 7.46 (d, 2H,  $J=7.2$  Hz, Ar- $H$ ), 7.39 (t, 1H,  $J=7.4$  Hz, Ar- $H$ ), 7.09-7.05 (m, 4H, Ar- $H$ ), 6.62 (d, 2H,  $J=8.0$  Hz, Ar- $H$ ), 6.53 (t, 1H,  $J=7.2$  Hz, Ar- $H$ ), 5.57 (t, 1H,  $J=6.0$  Hz, N- $H$ ), 5.15 (s, 2H, O- $\text{CH}_2$ ), 3.71 (t, 2H,  $J=6.2$  Hz, N- $\text{CH}_2$ ), 3.32-3.28 (m, 2H, N- $\text{CH}_2$ ).  $^{13}\text{C}$  NMR (100 MHz,  $\text{DMSO-d}_6$ )  $\delta$  (ppm): 161.5, 160.7, 149.2, 137.2, 129.9, 129.6, 129.3, 128.9, 128.4, 128.2, 116.1, 115.3, 112.6, 69.8, 60.0, 44.3. Elemental analysis (%): Calculated ( $\text{C}_{22}\text{H}_{22}\text{N}_2\text{O}$ ) (330,42) C,77.97; H,6.71; N,8.48; Found, C,77.10; H, 6.64; N, 8.39.

### 2.3.2 Synthesis of Pt(L)Cl<sub>2</sub>(Pt-L)



**Scheme 2.** Synthesis pathway for the Pt-L complex.

Ligand (L) (38.5 mg, 0.137 mmol) was dissolved in 2 mL of chloroform medium in a schlenk. Then, in a beaker,  $\text{Pt}(\text{DMSO})_2\text{Cl}_2$  (58 mg, 0.137 mmol) was prepared as a suspension in 3 mL chloroform medium and added dropwise onto Ligand L. The mixture was then stirred at reflux temperature for 72 hours. As a result of the reaction, the solvent volume was reduced until 1 mL of solution volume remained in the vacuum line and the solid was obtained by precipitation with 5 mL of diethyl ether. The light-yellow substance was dried under vacuum. Yield: 61%, Melting Point: 197 °C. FT-IR (KBr disk,  $\text{cm}^{-1}$ )  $\nu_{\text{C=N}}$  = 1599,  $\nu_{\text{Pt-Cl}}$  = 328 (with shoulder).  $^1\text{H}$  NMR (400 MHz,  $\text{DMSO-d}_6$ )  $\delta$  (ppm): 9.14 (s, 1H,  $\text{CH=N}$ ), 7.79-7.15 (m, 14H, Ar- $H$ ), 5.51(d, 1H, - $\text{NH}$ ), 5.20 (s, 2H, - $\text{CH}_2$ ), 4.09 (bs, 1H, N- $\text{CH}_2$ ), 3.92 (bs, 1H, N- $\text{CH}_2$ ), 3.03 (bs, 1H, N- $\text{CH}_2$ ), 2.77 (bs, 1H, N- $\text{CH}_2$ ).  $^{13}\text{C}$  NMR (100 MHz,  $\text{DMSO-d}_6$ )  $\delta$ (ppm): 165.8, 161.5, 146.5, 133.1, 129.4, 129.0, 128.3, 124.5, 124.3, 124.0, 115.8, 115.3, 112.5, 70.0, 61.1, 60.1, 46.0. Elemental analysis (%): Calculated ( $\text{C}_{22}\text{H}_{22}\text{Cl}_2\text{N}_2\text{OPt}$ )

(596,41) C,44.30; H,3.72; N,4.70; Found, C,43.81; H, 4.18; N, 4.08.

### 2.4. Thioflavin T Assay

Concentrations of the  $\text{A}\beta_{1-42}$  Aggregation Kit, purchased from AnaSpec, were prepared according to the kit procedure. For this purpose, stock solutions of complexes and  $\text{A}\beta_{1-42}$  prepared as specified in the biological measurements above were diluted with buffer containing 50mM Tris / 150mM NaCl, 20mM HEPES (4-(2-hydroxyethyl)-1-piperazinepropanesulfonic acid) / 150mM NaCl, 10mM Phosphate / 150mM NaCl and final concentrations 10  $\mu\text{M}$  for  $\text{A}\beta_{1-42}$  and 10  $\mu\text{M}$  for the complexes (corresponding to an interaction ratio of 1: 1) were prepared. The final DMSO concentration does not exceed 1 %. ThT solution prepared with buffer was adjusted to the final concentration of 42.6  $\mu\text{M}$ . It was determined by the literature data that an effective signal was obtained at this concentration (Xue et al. 2017).

Negative controls consisting of ThT and assay buffer and consisting of ThT-complex (Pt-L) was run to ensure that complex does not alter ThT fluorescence. Samples were plated in a black 96-well plate. The plate was sealed with aluminum sheets to prevent samples from light and kept in the dark. Fluorescence was measured through the plate bottom every 5 min for 165 min. at excitation 440 nm and emission 484 nm on a Thermo Fisher Scientific, Varioskan Flash microplate reader. Samples were kept at 37 °C under orbital agitation (550 rpm) in the plate reader between reads. Kinetic was plotted using GraphPad Prism.

### 2.5. Biological Activity

#### 2.5.1. Preparation of monomeric $\text{A}\beta_{1-42}$ and complexes stock solutions

Commercially purchased  $\text{A}\beta_{1-42}$  first interacted with HFIP, resolved, and published in accordance with the literature. This method primarily aimed to remove oligomers that may be present in commercial amyloid. Insoluble parts were separated by adding HFIP and the resulting solution was concentrated in a vacuum concentrator. Again, the literature was used to determine the concentration according to its effects (Ryan et al. 2013). It was then brought to the concentration to be studied by diluting with 1xPBS. In all measurements, amyloid solution was freshly prepared. Due to the low water solubility of the complexes, the complexes for the prepared stock solution were dissolved in 2:1 DMSO/ $\text{H}_2\text{O}$  medium and diluted to the targeted concentrations with phenol-free DMEM (Dulbecco's Modified Eagle Medium). In all cell measurements, an application method was followed in which the DMSO rate did not exceed 1%.

### 2.5.2. Cell culture studies

Human neuroblastoma cancer cell (SH-SY5Y) was used in cell culture studies. After removing the frozen cell from  $-80^{\circ}\text{C}$  in the cryotube. Then it was quickly thawed in a water bath and transferred to a flask and filled with DMEM medium. Phenol-red-free DMEM was selected as the medium used to determine the cytotoxicity levels of the cells, and all procedures were carried out under sterile conditions. The DMEM medium was prepared with 1% penicillin/streptomycin, 1% L-Glutamine, 1% non-essential amino acid, and 1% Sodium-pyruvate added to the bottle, and it was completed to 500 mL. For an optimal environment for cell growth, the cells were kept in an incubator at  $37^{\circ}\text{C}$ , containing 95% humidity and 5%  $\text{CO}_2$  conditions.

### 2.5.3. Cytotoxicity studies

In 96-well plates,  $1 \times 10^5$  SH-SY5Y cells (for 72 hours) were seeded in each well. To determine the cytotoxicity of the complexes alone, master stock solutions of the complexes were diluted with DMEM to the obtained concentrations and added to the wells at (0.1;0.5;1;10;50;100)  $\mu\text{M}$  concentrations. After 72 hours of cell cultivation, the medium was removed from the cells and the wells were washed 2 times with 1x PBS. At the end of the relevant time, the medium was removed from the cells, 100  $\mu\text{L}$  of 0.5 mg/mL MTT (3-(4,5-Dimethylthiazol-2-yl)-2,5-diphenyltetrazolium bromide) was added to each well and incubated at  $37^{\circ}\text{C}$  for 3 hours. After the incubation was completed, the medium with MTT was removed from each well and 150  $\mu\text{L}$  of DMSO (Dimethyl sulfoxide) was added to dissolve the MTT crystals in the cell. The absorbance of the wells was measured at 570 nm with a microplate reader (Thermo Scientific, Varioskan Flash). The percent viability of the control group (untreated group) was considered 100% and the ab-

sorption value of each well was calculated as a percentage relative to the control group, and the experiments were repeated three times.

As a result of this study, the inhibitory effect of the complexes on the toxicity of  $\text{A}\beta_{1-42}$  in neuronal cell culture was determined by MTT measurement. Neuronal cells were incubated with  $\text{A}\beta_{1-42}$  for 72h (Interaction with HFIP (Hexafluoroisopropanol) may give erroneous results for the first 24 hours with a final concentration of 10  $\mu\text{M}$  in the presence of complexes at concentrations of 10 and 5  $\mu\text{M}$  respectively.

After removing the medium from the installation, 0.5 mg/mL MTT was added to the wells and incubated at  $37^{\circ}\text{C}$  for 3 hours. After the incubation period was completed, the medium with MTT was removed from each well and 150  $\mu\text{L}$  of DMSO was added to open the MTT crystal cells inside. The absorbance of the wells was measured at 570 nm with a microplate reader and again compared with the control group to calculate the percentage of cell viability (Mosmann 1983).

## 3. Results and Discussion

### 3.1. Synthesis Studies of Ligands and Complexes

Synthesis schemes of the ligand and complex are shown in Schemes 1 and 2, and  $^1\text{H}$  NMR and  $^{13}\text{C}$  NMR spectra of the ligand and complex are given in Figures 1, 2, 3 and 4, respectively.

$^1\text{H}$  NMR and  $^{13}\text{C}$  NMR spectra of L and complex Pt-L were recorded in  $\text{DMSO-d}_6$  media according to their solubility. The imine peak seen at 8.25 ppm in the ligand shifted to 9.14 ppm with complex formation. The signal of the  $\text{CH}_2$  group bound to oxygen in the ligand shifted from 5.15 ppm

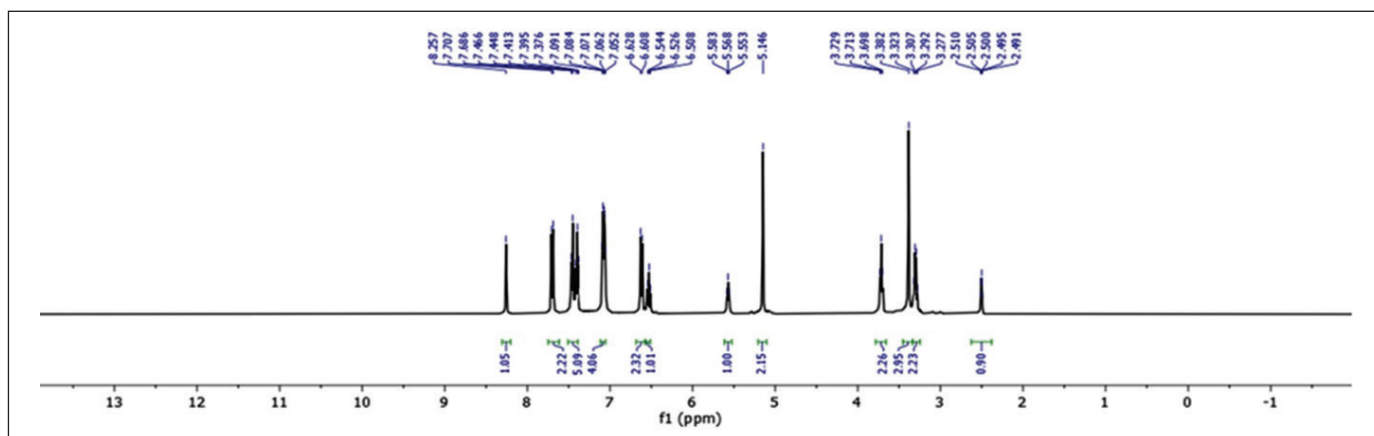


Figure 1.  $^1\text{H}$ -NMR spectrum of Ligand (L).

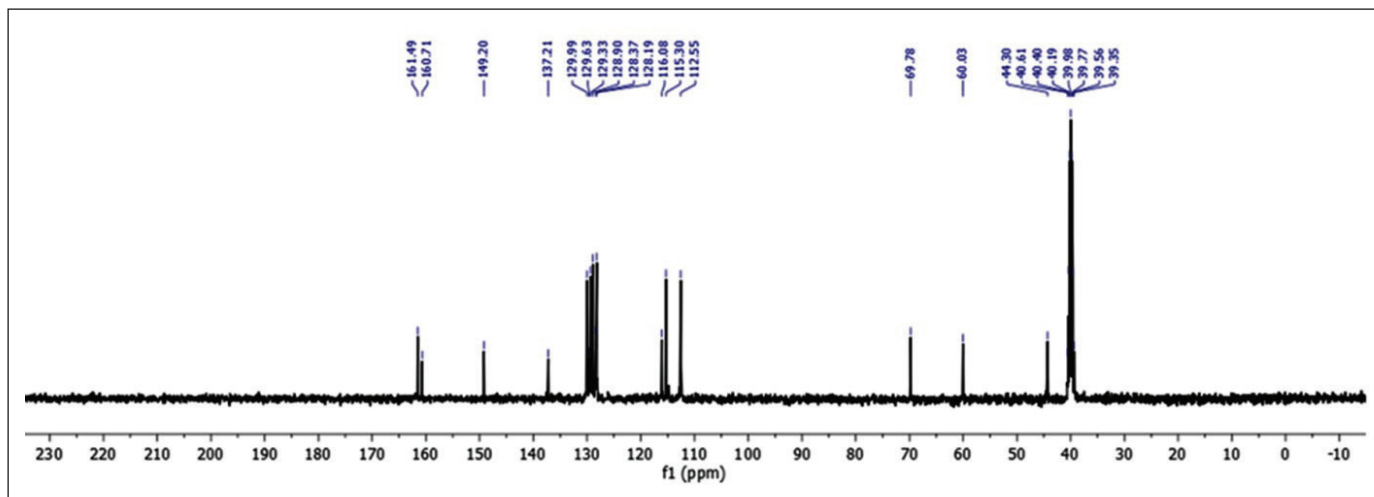


Figure 2.  $^{13}\text{C}$ -NMR spectrum of Ligand (L).

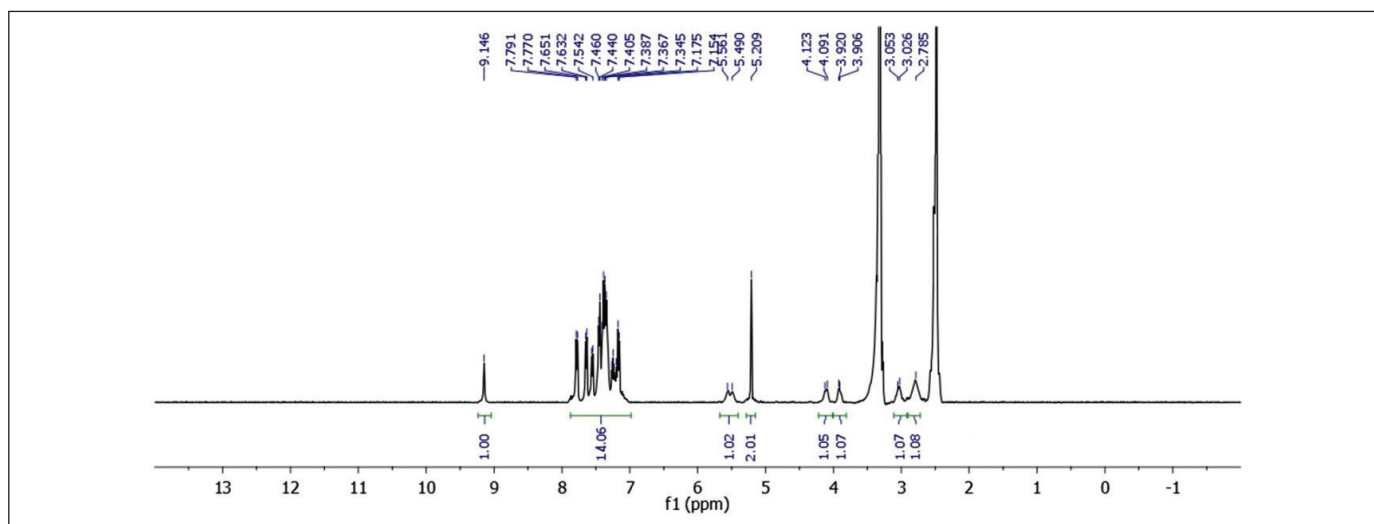


Figure 3.  $^1\text{H}$ -NMR spectrum of complex (Pt-L).

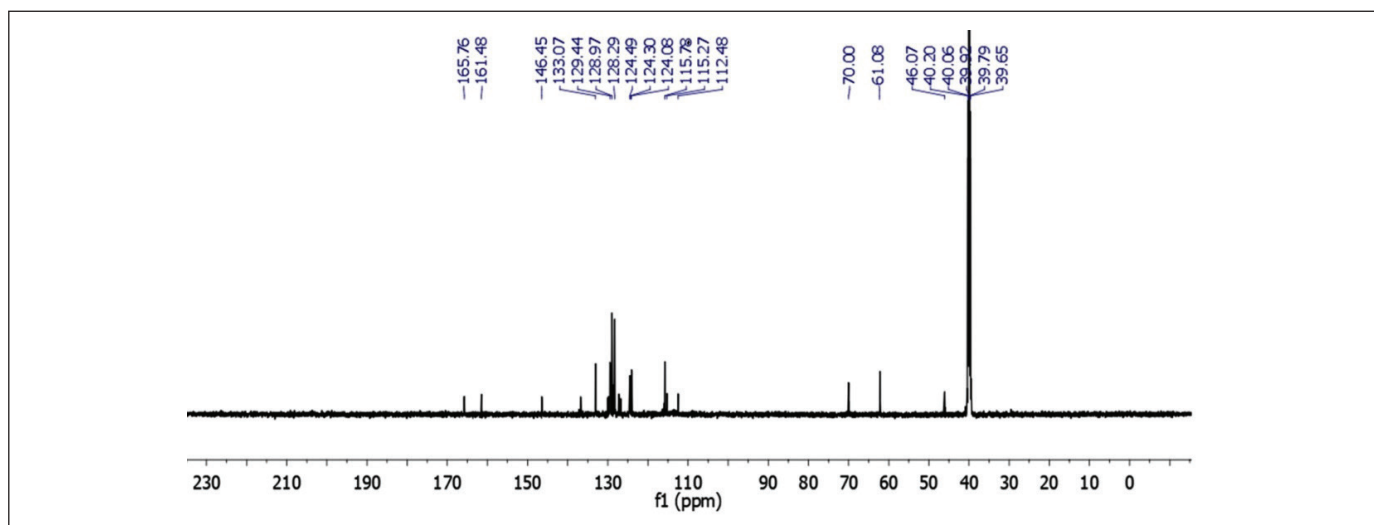


Figure 4.  $^{13}\text{C}$ -NMR spectrum of complex (Pt-L).

to 5.20 ppm with complex formation. The proton signal of the CH<sub>2</sub> group bound to nitrogen is seen as a singlet at 3.71 ppm in the free ligand, while it is observed as two separate singlets at 3.92 and 4.09 ppm with complex formation. When the <sup>1</sup>H NMR and <sup>13</sup>C NMR spectra for L and Pt-L are examined, shifts are seen relative to the free ligand. In particular, the characteristic imine proton (N=CH) and imine carbon (N=CH) shifts to higher ppm from the free ligand indicated that the complex were imine bound (Miles et al. 2016, Patterson *et al.* 2014, Shiju et al. 2015). The peaks of the protons in the CH<sub>2</sub> group are also seen by separating them in ligand spectrum (Damoc et al. 2020). A shift in CH<sub>2</sub> protons was observed relative to the free ligand in the

complex spectrum. The results of the NMR assessments are presented in Table 1.

The FT-IR spectra of the complex obtained was compared with the ligand. This spectrum shows that the  $\nu_{(C=N)}$  modes change with complexation. While there is a clear distinction in *cis*- Pt-Cl peaks of the starting complex [PtCl<sub>2</sub>(DM-SO)<sub>2</sub>], it was observed as a peak containing a shoulder in the FT-IR spectra of the Pt-L complex (Figure 6 and 7). However, when the literature data are examined, it is seen that this distinction is not fully observed in some *cis*-structured complexes (Gümüş et al. 2009).

Elemental analysis results of the ligand and complex are compatible with the suggested structure.

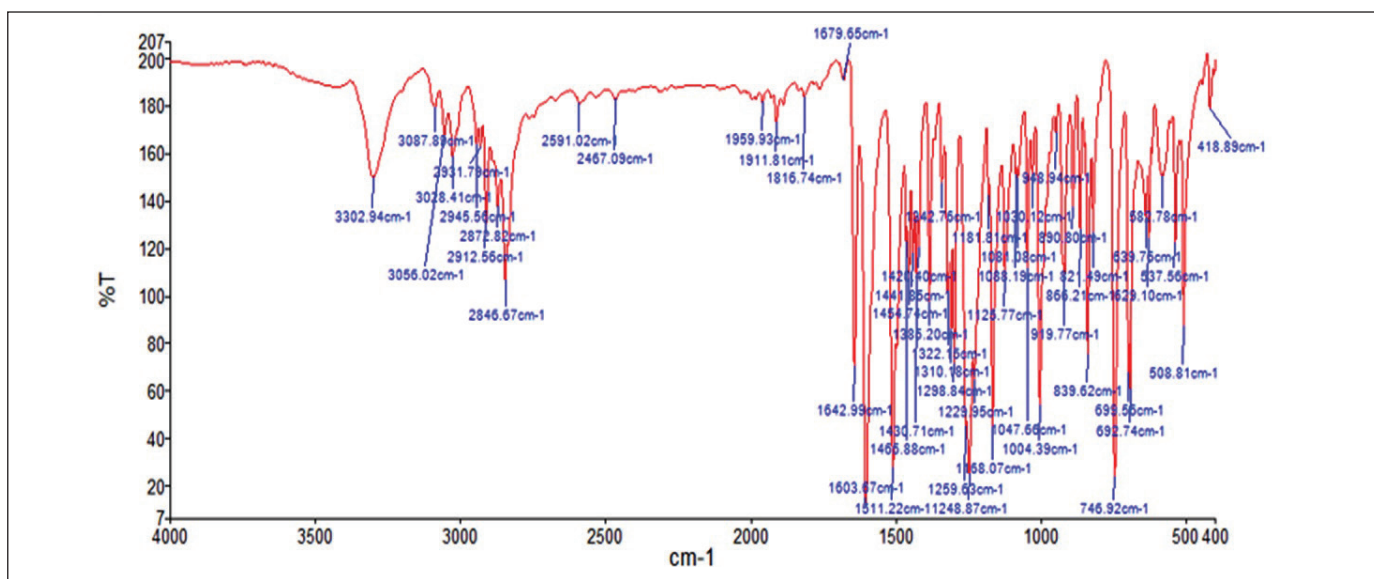


Figure 5. FT-IR spectrum of Ligand (L).

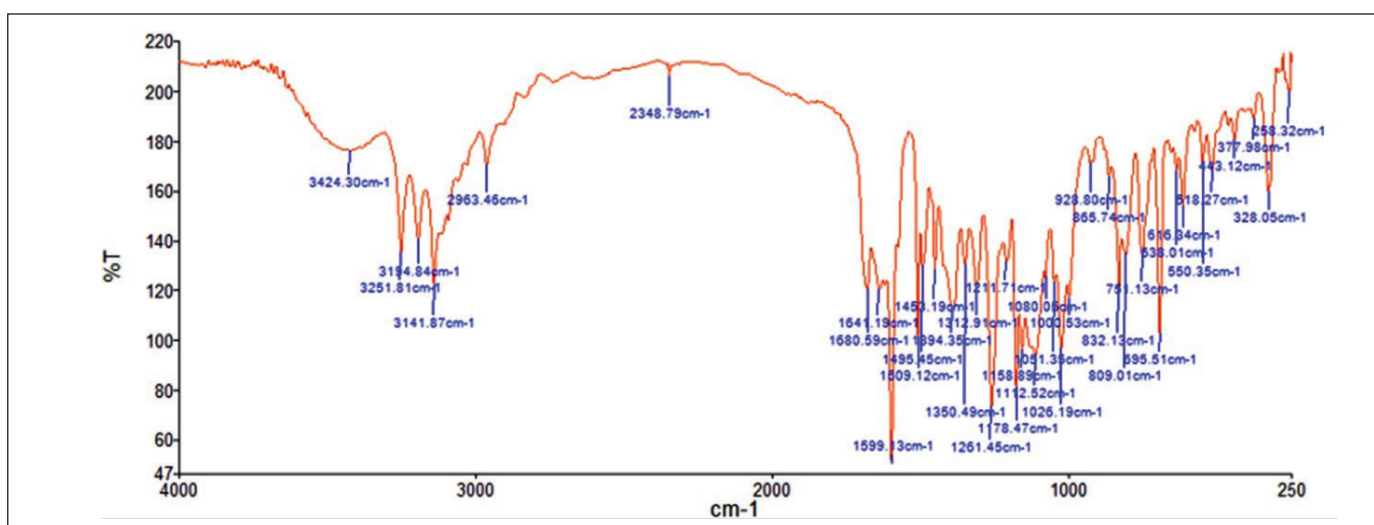


Figure 6. FT-IR spectrum of complex (Pt-L).

**Table 1:**  $^1\text{H}$ - and  $^{13}\text{C}$ -NMR peak assignments for ligand and complex.

| Ligand (L)           |               | complex (Pt-L)   |                                  |
|----------------------|---------------|--|----------------------------------|
|                      |               |  |                                  |
| $^1\text{H}$ -NMR    |               |  |                                  |
| Number               | ppm           | Number   | ppm                              |
| 15                   | 8.25 (s)      | 15   | 9.14                             |
| 2, 6                 | 7.69 (d)      | 2, 3, 5, 6, 10, 11, 12,<br>13, 14, 21, 22,<br>23, 24, 25 | 7.79-7.15 (m)                    |
| 3, 5                 | 7.46 (d)      |  |                                  |
| 11, 13               | 7.39 (t)      |  |                                  |
| 10, 12, 14, 21, 25   | 7.09-7.05 (m) |  |                                  |
| 22, 24               | 6.62 (d)      |  |                                  |
| 23                   | 6.53 (t)      |  |                                  |
| 19                   | 5.57 (bs)     | 19   | 5.51 (bs)                        |
| 8                    | 5.15 (s)      | 8  | 5.20 (s)                         |
| 17                   | 3.71 (t)      | 17   | 4.09 (bs) (1H)<br>3.92 (bs) (1H) |
| 18                   | 3.32-3.28 (m) | 18   | 3.03 (bs) (1H)<br>2.77 (bs) (1H) |
| $^{13}\text{C}$ -NMR |               |  |                                  |
| Number               | ppm           | Number   | ppm                              |
| 4                    | 161.5         | 4  | 165.8                            |
| 15                   | 160.7         | 15   | 161.5                            |
| 20                   | 149.2         | 20   | 146.5                            |
| 9                    | 137.2         | 9  | 133.1                            |
| 2, 6                 | 129.9         | 2, 6   | 129.4                            |
| 22, 24               | 129.6         | 22, 24   | 129.0                            |
| 1                    | 129.3         | 1  | 128.3                            |
| 11, 13               | 128.9         | 11, 13   | 124.5                            |
| 12                   | 128.4         | 12   | 124.3                            |
| 10, 14               | 128.2         | 10, 14   | 124.0                            |
| 23                   | 116.1         | 23   | 115.8                            |
| 21, 25               | 115.3         | 21, 25   | 115.3                            |
| 3, 5                 | 112.6         | 3, 5   | 112.5                            |
| 8                    | 69.8          | 8  | 70.0                             |
| 17                   | 60.0          | 17   | 61.1                             |
| 18                   | 44.3          | 18   | 46.0                             |

\*s: singlet; d: doublet; t: triplet; m: multiplet; bs: broad singlet.

### 3.2. Biological Assessment

#### 3.2.1. Determination of cytotoxic activities of complex

The cytotoxicity of the complex was studied for 72 hours (Figure 7). The initial concentration was determined as 10  $\mu\text{M}$  (Yellol et al. 2015). The cytotoxicity of the complex for  $\text{IC}_{50}$  value over 72 hours is 19.22  $\mu\text{M}$ .

After determination and evaluation of the cytotoxicity of the complex alone in the SH-SY5Y cell line, the appropriate concentration was determined for cytotoxicity studies to be measured by  $\text{A}\beta_{1-42}$ . The concentration of the complex was determined to correspond to the molar ratio of 1.0:1.0 and 1.0:0.5 amyloid/complex.  $\text{A}\beta_{1-42}$  alone was added to the medium as a control (Figure 5).

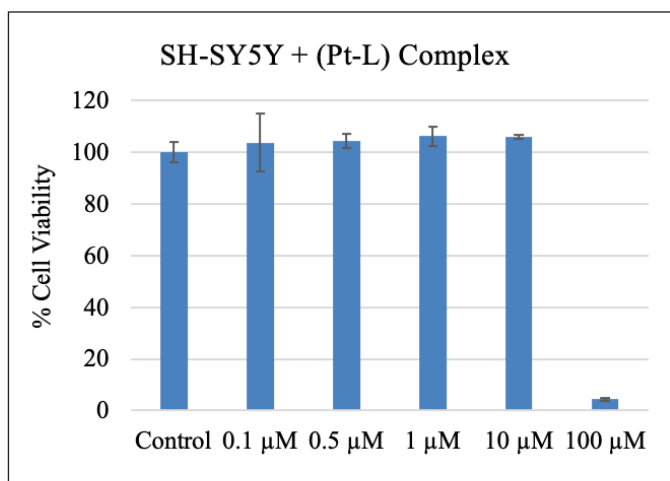


Figure 7. Cytotoxicity of the Pt-L on the cell viability

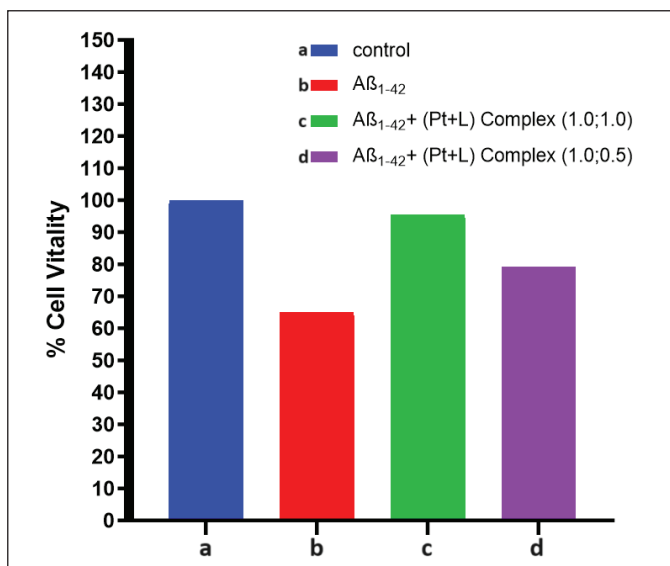


Figure 8. Inhibition of the  $\text{A}\beta_{1-42}$  toxicity.

After 72 hours (Vyas et al. 2018) 10  $\mu\text{M}$ .  $\text{A}\beta_{1-42}$  was found to have approximately 65% cell viability by measurements, which is consistent with literature data (Kristhal et al. 2019). Interactions of the complexes with amyloid at 1:1 and 1:0.5 molar ratios were also performed over 72 hours.

As seen in the Figure 8, because of the findings, it was observed that the complex at both molar ratios inhibited the cytotoxicity caused by  $\text{A}\beta_{1-42}$  aggregation.

It showed higher activity in 1.0: 1.0 molar ratio than 1.0:0.5 in 1 molar ratio. This is compatible with some literature data (Roberts et al. 2020). When the studies on Pt complexes were examined, it was observed that certain activation was obtained at 1.0:2.0 amyloid/complex ratios in general. The result determined for the complex in this study appears to be lower than the metal molar ratio found in many other studies (Messori et al. 2013).

#### 3.3. Thioflavine-T Aggregation Inhibition Studies

One of the most common method used to determine the aggregation kinetics of  $\text{A}\beta_{1-42}$  is the Thioflavine-T fluorescence measurement technique. As a control,  $\text{A}\beta_{1-42}$  in the medium showed an increase in fluorescence over time. To determine the  $\text{A}\beta_{1-42}$  / complex interaction ratio, measurements with  $\text{A}\beta_{1-42}$  / complex molar ratios of 1.0:1.0 and 1.0: 0.5 were made. The results are given in Fig 9a and 9b. As a result of this measurement, it was observed that the interaction of 1.0:1.0 molar ratio inhibited amyloid aggregation more than other ratio. Compared with literature data, the complexes we examined show a lower molar ratio (Messori et al. 2013, Lu et al. 2015) suggesting that they are more active in amyloid aggregation. By analyzing the area under the curve, it can be calculated that complex (1.0:1.0 molar ratio) interacts with amyloide at a rate of 65%.

There are only three studies conducted with Schiff bases in the literature (Heffern et al. 2014, Roberts et al. 2020, Iscen et al. 2019), and the effect of only one Co-Schiff base complexes on the aggregation of  $\text{A}\beta_{1-42}$  was examined and it was reported that the compound they synthesized interacted with amyloid at a rate of approximately 70% (Roberts et al. 2020). In studies available in the literature, the values generally found for the compounds examined in fluorescence measurement data are those with a similar effect in the molar ratio of 1.0:2.0 (amyloid/complex) (Roberts et al. 2020, Messori et al. 2013, Lu et al. 2015). In a few studies, the interaction ratio is 1.0:1.0 (Vyas et al. 2018, Florio et al. 2020). These results obtained in our study show that complex Pt-L is promising in terms of inhibition of  $\text{A}\beta_{1-42}$ .



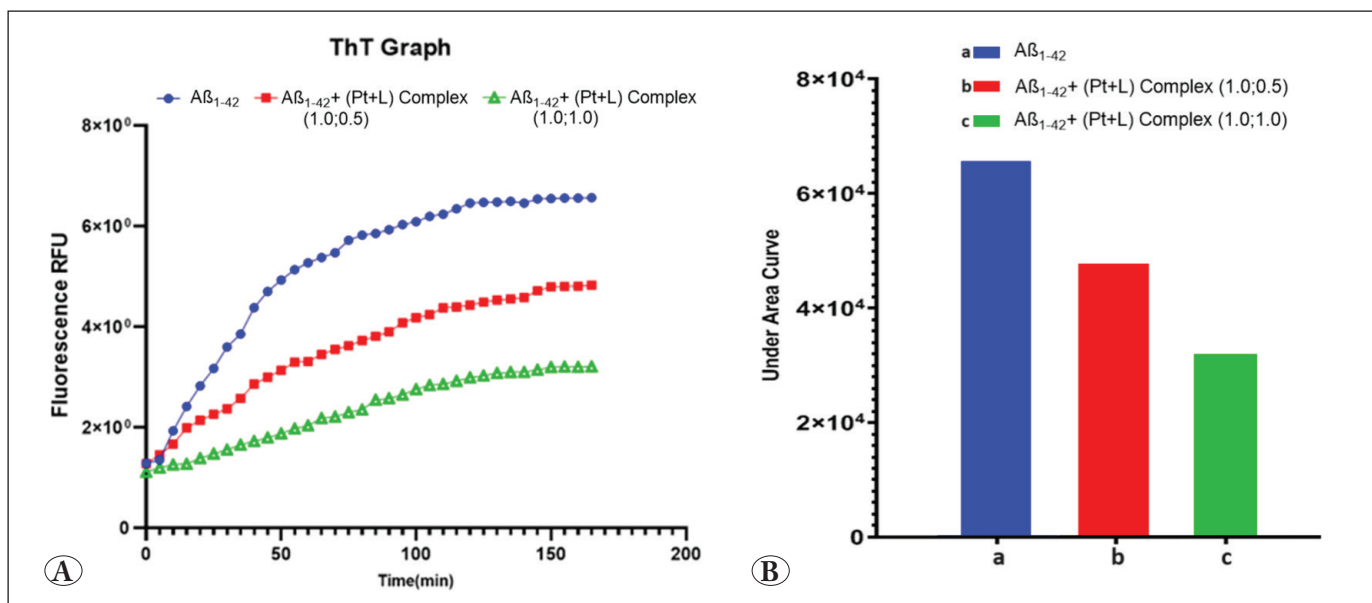


Figure 9. A) Fluorescent graphic. B) Under the curve Area.

#### 4. Conclusion and Suggestions

In this study, the synthesis of a new amine/imine structured Schiff base and its chelated platinum complex is reported. The structures of the ligand and the complex were elucidated by spectroscopic methods. The cytotoxicity of the complex on SH-SY5Y neuroblastoma cells was examined and its  $IC_{50}$  value was found as 19.22  $\mu\text{M}$ .

The activation of the complex on the cells with amyloid was measured by determining the non-toxic concentration. It has been determined that it inhibits amyloid aggregation and increases cell viability, especially when the amyloid/complex is in a 1.0:1.0 molar ratio. Again, with the help of fluorescence measurements, it was understood that the complex interacts with 65% of the amyloid. These results obtained in our study show that the complex is promising in terms of inhibition of  $A\beta_{1-42}$ .

#### 5. References

- Damoc, M., Stoica, AC., Macsim, A., Dascalu, M., Zaltariov, M., Cazacu, M. 2020.** Salen-type schiff bases spaced by the highly flexible and hydrophobic tetramethyldisiloxane motif. Some synthetic, structural and behavioral particularities. *Journal of Molecular Liquids*, 2020, 316, 113852-113863. Doi: 10.1016/j.molliq.2020.113852
- Florio, D., Cuomo, M., Iacobucci, I., Ferraro, G., Mansour, AM., Monti, M., Merlino, A., Marasco, D. 2020.** Complexes modulation of amyloidogenic peptide aggregation by photoactivatable CO-releasing ruthenium(II) complexes. *Pharmaceuticals*, 8, 171-183. Doi: 10.3390/ph13080171
- Gaetke, LM., ChowJohnson, HS., Chow, C.K. 2014.** Copper: toxicological relevance and mechanisms. *Archives of Toxicology*, 88, 1929-1938. Doi: 10.1007/s00204-014-1355-y
- Garai, M., Das, A., Joshi, M., Paul, S., Shit, M., Choudhury, AR., Biswas, B. 2018.** Synthesis and spectroscopic characterization of a photo-stable tetrazinc (II)-Schiff base cluster: A rare case of ligand centric phenoxazinone synthase activity. *Polyhedron*, 156, 223-230. Doi: 10.1016/j.poly.2018.09.044
- Gümüş, F., Eren, G., Açıık, L., Çelebi, A., Öztürk, F., Yılmaz, Ş., Sağkan, RI., Gür, S., Özkul, A., Elmalı, A., Elerman, Y. 2009.** Synthesis, cytotoxicity, and dna interactions of new cisplatin analogues containing substituted benzimidazole ligands. *Journal of Medicinal Chemistry*, 52, 1345-1357. Doi: 10.1021/jm8000983
- Haas, A. 1971.** The synthesis and characterization of inorganic compounds. *Angewandte Chemie*, 83,220-220. Doi: 10.1002/ange.19710830622.
- Heffern, MC., Velasco, PT., Matosziuk, LM., Coomes, JL., Karras, C., Ratner, MA., Klein, WI., Eckermann, AL., Meade, TJ. 2014.** Modulation of amyloid- $\beta$  aggregation by histidine-coordinating Cobalt(III) schiff base complexes. *ChemBioChem Communications*, 15, 1584-1589. Doi: 10.1002/cbic.201402201

- Iscen, A., Brue, CR., Roberts, KF., Kim, J., Schatz, GC., Meade, TJ. 2019.** Inhibition of amyloid- $\beta$  aggregation by cobalt(III) Schiff base complexes: A computational and experimental approach. *Journal of the American Chemical Society*, 141, 16685-16695. Doi: 10.1021/jacs.9b06388.
- Kepp, KP. 2017.** Alzheimer's disease: How metal ions define  $\beta$ -amyloid function. *Coordination Chemistry Reviews*, 351, 127-159. Doi: 10.1016/j.ccr.2017.05.007
- Khan, HY., Ahmad, A., Hassan, MN., Khan, YH., Arjmand, F., Khan, RH. 2024.** Advances of metallodrug-amyloid  $\beta$  aggregation inhibitors for therapeutic intervention in neurodegenerative diseases: Evaluation of their mechanistic insights and neurotoxicity. *Coordination Chemistry Reviews*, 501, 215580-215599. Doi: 10.1016/j.ccr.2023.215580
- Krishtal, J., Metsla, K., Bragina, O., Tougu, V., Palumaa, P. 2019.** Toxicity of amyloid- $\beta$  peptides varies depending on differentiation route of SH-SY5Y cells. *Journal of Alzheimer Disease*, 71, 879-887. Doi: 10.1016/j.jpharm.2018.07.046
- Liu, HY., Li, C., Ma, JJ. 2014.** New Vanadium and Zinc Complexes with Schiff Base Ligand N,N'-bis(3-Ethoxy-2-Hydroxybenzylidene)ethylenediamine: Synthesis, Structures, and biochemical properties. *Russian journal Coordination Chemistry*, 40, 240-245. Doi: 10.1134/S1070328414040046
- Liu, H., Qu, Y., Wang, X. 2018.** Amyloid  $\beta$ -targeted metal complexes for potential applications in Alzheimer's disease. *Future Medicinal Chemistry*, 10, 1756-8919. Doi: 10.4155/fmc-2017-0248
- Lu, L., Zhong, HJ., Wang, M., Ho, SL., Li, HW., Leung, CH., Ma, DL. 2015.** Inhibition of beta-amyloid fibrillation by luminescent iridium (III) complex probes. *Scientific reports*, 5, 14619. Doi: 10.1038/srep14619
- Messori, L., Camarri, M., Ferraro, T., Gabbani, C., Franceschini, D. 2013.** Promising in vitro anti-alzheimer properties for a ruthenium(III) complex. *ACS Medicinal Chemistry Letters*, 4, 329-332. Doi: 10.1021/ml3003567
- Miles, BA., Patterson, AE., Vogels, CM., Decken, AJ., Waller, C., Morin, PJ., Westcott, SA. 2016.** Synthesis, characterization, and anticancer activities of lipophilic pyridinecarboxaldimine platinum(II) complexes. *Polyhedron*, 108, 23-29. Doi: 10.1016/j.poly.2015.07.039
- Mohammed, GG., Omar, MMA., Moustafa, BS., Abdel-Halim, HF., Farag, NA. 2022.** Spectroscopic investigation, thermal, molecular structure, antimicrobial and anticancer activity with modelling studies of some metal complexes derived from isatin Schiff base ligand. *Inorganic Chemistry Communications*, 141, 109606-109619. Doi: 10.1016/j.inoche.2022.109606
- Mosmann, T. 1983.** Rapid colorimetric assay for cellular growth and survival: application to proliferation and cytotoxicity assays. *Journal of Immunological Methods*, 65, 55-63. Doi: 10.1016/0022-1759(83)90303-4.
- Pal, CK., Mahato, S., Joshi, M., Paul, S., Choudhury, AR., Biswas, B. 2020.** Transesterification activity by a zinc(II)-Schiff base complex with theoretical interpretation. *Inorganic Chimica Acta*, 506, 119541. Doi: 10.1016/j.ica.2020.119541
- Palanimuthu, D., Poon, R., Sahni, S., Anjum, R., Hibbs, D., Lin, HY., Bernhardt, PV., Kalinowski, DS., Richardson, DR. 2017.** A novel class of thiosemicarbazones show multifunctional activity for the treatment of Alzheimer's disease. *European Journal of Medicinal Chemistry*, 139, 612-632. Doi: 10.1016/j.ejmech.2017.08.021
- Patterson, AE., Miller, JJ., Miles, BA., Stewart, EL., Melanson, JM., Vogels, EJ., Cockshutt, CM., Decken, AM., Morin, A., Westcott, PJ. 2014.** Synthesis, characterization and anticancer properties of (salicylaldiminato) platinum(II) complexes. *Inorganica Chimica Acta*, 415, 88-94. Doi: 10.1016/j.ica.2014.02.028
- Price, JH., Williamson, AN., Schramm, RF., Wayland, BB., 1972.** Palladium(II) and platinum(II) alkyl sulfoxide complexes. Examples of sulfur-bonded, mixed sulfur- and oxygen-bonded, and totally oxygen-bonded complexes. *Inorganic Chemistry*, 11, 1280-1284. Doi: 10.1021/ic50112a025
- Rao, PS., Kurumurthy, C., Veeraswamy, B., Kumar, GS., Narsaiah, B., Kumar, KP., Murthy, USN., Karnewar, S., Kotamraju, S. 2013.** Synthesis, antimicrobial and cytotoxic activities of novel 4-trifluoromethyl-(1,2,3)-thiadiazolo-5-carboxylic acid hydrazide Schiff's bases. *Medicinal Chemistry Research*, 22, 1747-1755. Doi: 10.1007/s00044-012-0168-x
- Roberts, KF., Brue, CR., Preston, A., Baxter, D., Herzog, E., Varelas, E., Meade, TJ. 2020.** Cobalt(III) Schiff base complexes stabilize non-fibrillar amyloid- $\beta$  aggregates with reduced toxicity. *Journal of Inorganic Biochemistry*, 213, 111265. Doi: 10.1016/j.jinorgbio.2020.111265
- Ross, CA., Poirier, MA. 2004.** Protein aggregation and neurodegenerative disease. *Nature Medicine*, 10, 10-17. Doi: 10.1038/nm1066
- Rowinska-Zyrek, M., Salerno, M., Kozlowski, H. 2015.** Neurodegenerative diseases - Understanding their molecular bases and progress in the development of potential treatments. *Coordination Chemistry Reviews*, 284, 298-312. Doi: 10.1016/j.ccr.2014.03.026
- Ryan, TM., Caine, J., Mertens, HDT., Kirby, N., Nigro, J., Breheny, K., Waddington, LJ., Strelsov, VA., Curtain, C., Masters, CL., Robert, BR. 2013.** Ammonium hydroxide treatment of  $a\beta$  produces an aggregate free solution suitable for biophysical and cell culture characterization. *Peerj*, 73, 1-20. Doi: 10.7717/peerj.73

- Santos, MA., Chand, K., Chaves, S. 2016.** Recent progress in multifunctional metal chelators as potential drugs for Alzheimer's disease. *Coordination Chemistry Reviews*, 327-328, 287-303. Doi: 10.1016/j.ccr.2016.04.013
- Shiju, C., Arish, D., Bhuvanesh, N. Kumaresan, S. 2015.** Synthesis characterization and biological evaluation of schiff base-platinum(II) complexes. *Spectrochimica Acta, Part A: Molecular and Biomolecular Spectroscopy*, 145, 213-222. Doi: 10.1016/j.saa.2015.02.030
- Soto, C., Pritzkow, S. 2018.** Protein misfolding, aggregation, and conformational strains in neurodegenerative diseases. *Nature Neuroscience*, 21, 1332-1340. Doi: 10.1038/s41593-0180235-9
- Valensin, D., Gabbani, C., Messori, L. 2012.** Metal compounds as inhibitors of  $\beta$ -amyloid aggregation. Perspectives for an innovative metallotherapeutics on Alzheimer's disease. *Coordination Chemistry Reviews*, 256, 2357-2366. Doi: 10.1016/j.ccr.2012.04.010
- Vyas, NA., Singh, SB., Kumbhar, AS., Ranade, DS., Walke, GR., Kulkarni, PP., Jani, V., Sonavane, UB., Joshi, RR., Rapole, S. 2018.** Acetylcholinesterase and A $\beta$  aggregation inhibition by heterometallic ruthenium(II)-platinum(II) polypyridyl complexes. *Inorganic Chemistry*, 57, 7524-7535. Doi: 10.1021/acs.inorgchem.8b00091
- Xue, C., Lin, TY., Chang, D., Guo, Z. 2017.** Thioflavin T as an amyloid dye: fibril quantification, optimal concentration, and effect on aggregation, *Royal Society Open Science*, 4, 160696-160708. Doi: 10.1098/rsos.160696
- Yello, GS., Yello, JG., Kenche, VB., Liu, XM., Barnham, KJ., Donaire, A., Janiak, C., Ruiz, J. 2015.** Synthesis of 2-pyridyl-benzimidazole iridium(III), ruthenium(II), and platinum(II) complexes. study of the activity as inhibitors of amyloid- $\beta$  aggregation and neurotoxicity evaluation. *Inorganic Chemistry*, 54, 470-475. Doi: 10.1021/ic502119b